ORIGINAL RESEARCH

Specific Binding of Novel SPION-Based System Bearing Anti-N-Cadherin Antibodies to Prostate Tumor Cells

Karolina Karnas[1,2]
Tomasz Strączek[3]
Czesław Kapusta[3]
Małgorzata Lekka[4]
Joanna Dulińska-Litewka [ID][2]
Anna Karewicz [ID][1]

[1]Department of Chemistry, Jagiellonian University, Kraków, Poland; [2]Chair of Medical Biochemistry, Jagiellonian University Medical College, Kraków, Poland; [3]AGH University of Science and Technology, Faculty of Physics and Applied Computer Science, Department of Solid State Physics, Kraków, Poland; [4]Department of Biophysical Microstructures, Institute of Nuclear Physics, Polish Academy of Sciences, Kraków, Poland

Purpose: Epithelial–mesenchymal (EMT) transition plays an important role in metastasis and is accompanied by an upregulation of N-cadherin expression. A new nanoparticulate system (SPION/CCh/N-cad) based on superparamagnetic iron oxide nanoparticles, stabilized with a cationic derivative of chitosan and surface-modified with anti-N-cadherin antibody, was synthetized for the effective capture of N-cadherin expressing circulating tumor cells (CTC).

Methods: The morphology, physicochemical, and magnetic properties of the system were evaluated using dynamic light scattering (DLS), fluorescence spectroscopy, Mössbauer spectroscopy, magnetometry, and fluorescence spectroscopy. Atomic force microscopy (AFM), confocal microscopy and flow cytometry were used to study the interaction of our nanoparticulate system with N-cadherin expressed in prostate cancer cell lines (PC-3 and DU 145). A purpose-built cuvette was used in the cancer cell capture experiments.

Results: The obtained nanoparticles were a spherical, stable colloid, and exhibited excellent magnetic properties. Biological experiments confirmed that the novel SPION/CCh/N-cad system interacts specifically with N-cadherin present on the cell surface. Preliminary studies on the magnetic capture of PC-3 cells using the obtained nanoparticles were successful. Incubation times as short as 1 minute were sufficient for the synthesized system to effectively bind to the PC-3 cells.

Conclusion: Results obtained for our system suggest a possibility of using it to capture CTC in the flow conditions.

Keywords: superparamagnetic iron oxide nanoparticles, N-cadherin, antibody, circulating tumor cells, cancer, magnetic cell capture

Introduction

Metastasis is the leading cause of cancer-related deaths, with at least 70% of the solid cancers related death being attributed to its occurrence.[1] Early detection of the ongoing metastatic processes is therefore vital for patient's prognosis and optimal treatment strategy. Finding a way to prevent or hinder the formation of secondary tumors is still the largest challenge in cancer therapy, mainly due to the complexity of the processes involved. The changes in the cell–cell and cell–matrix adhesion play a central role in all stages of the metastatic cascade: invasion, intravasation, migration and extravasation.[2] The detachment and migration of the cells from the primary tumor are enabled by the change in their phenotype known as EMT. It permits the polarized, epithelial cells to go through a series of biochemical and morphological processes, shifting them to the more invasive, mesenchymal phenotype with enhanced migratory properties.[3] Such cells, known as CTC, can enter the bloodstream and migrate, spreading cancer to distant

Correspondence: Anna Karewicz
Department of Chemistry, Jagiellonian University, Gronostajowa 2, Kraków, 30-387, Poland
Tel +48 12 686 25 33
Fax +48 12 686 27 50
Email karewicz@chemia.uj.edu.pl

Joanna Dulińska-Litewka
Chair of Medical Biochemistry, Jagiellonian University Medical College, Kopernika 7, Kraków, 31-034, Poland
Tel +48 12 422 74 00
Fax +48 12 422 32 72
Email joanna.dulinska-litewka@uj.edu.pl

Graphical Abstract
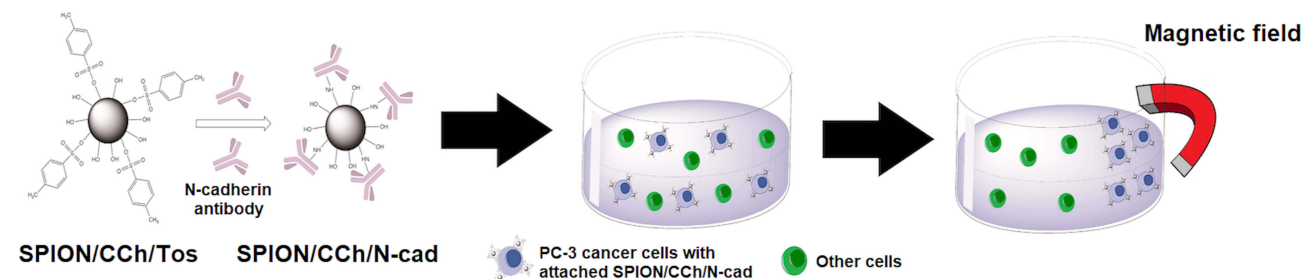
locations. Targeting, capturing, and analyzing the captured CTC allows for a more precise estimation of patient's prognosis, for monitoring cancer progression or recurrence, and may in the future allow to prevent, limit, or at least slow down metastasis.

Cadherins are calcium-dependent transmembrane proteins involved in regulating cell–cell adhesion,[4] which have a pivotal role in metastasis. A combined downregulation of E-cadherin and upregulation of N-cadherin expression, known as cadherin switching, is a hallmark of tumor aggressiveness.[3] It is also typical for the cells undergoing EMT.[5] When human pancreatic cancer cells (BxPC-3) were injected into the pancreas of nude mice, they upregulated N-cadherin expression and produced invasive tumors.[6] However, when a dedicated short hairpin RNA was used to abolish N-cadherin expression in these cells, they produced non-invasive tumors. The results of Hazan et al[7] showed that N-cadherin expression in metastatic breast cancer cells promotes tumor cell clustering and enhances their association with surrounding stroma, facilitating their invasion. An increase in N-cadherin expression was shown to occur in various types of metastatic cancer, including prostate,[8] breast,[9] and pancreatic[10] cancer, as well as melanoma.[11] It seems, therefore, to be a promising target for CTC detection and capture.

Among different methodologies developed to target or/and capture CTC, the most widely approved are those based on either the biophysical properties of CTC or immunoaffinity assays using specific biomarkers; the latter being the only Food and Drug Administration approved strategy of CTC detection to date.[12] This method is based on the use of antibodies specifically binding to the biomarkers expressed on the surface of CTC. Most of the technologies designed to capture CTCs derived from epithelial tumors target the epithelial cell adhesion molecule (EpCAM).[13] The prognostic significance of EpCAM+/CK+/CD45-configuration, where CD45 is a common leukocyte antigen and CK is cytokeratin, was already confirmed. There are, however, new data emerging that confirm the heterogeneity of the CTC population, including the existence of EpCAM- and/or CK-phenotypes.[14–16] The importance of EMT and stem cell markers in CTC capture is therefore recently gaining more attention. Researchers have expanded the range of specific antigens used in immunoaffinity-based capture, including stem cell markers (eg CD133 antigen (prominin-1)) and mesenchymal markers (eg cell-surface vimentin (CSV)).[17] N-cadherin, being a well-established marker of EMT, is another promising candidate.

Superparamagnetic iron oxide nanoparticles (SPION) are widely studied in the context of anti-cancer therapies.[18–20] They may be applied as Magnetic Resonance Imaging (MRI) contrast agents in tumor visualization, as nanocarriers for drug delivery, in magnetic hyperthermia, or for magnetic capture of CTC. One of the main concerns considering the biological application of SPION is their tendency to aggregate. A possible solution is to coat their surface with a thin polymeric layer. Zapotoczny et al[21] have synthetized cationic derivative of chitosan (CCh) where some of the amine groups were substituted with trimethylammonium units and used it to coat SPION. The resulting SPION/CCh nanoparticles had a high positive charge in a wide range of pH and thus were colloidally stable; they also showed excellent magnetic properties.[22,23] These SPION were then further functionalized to obtain MRI contrasts specifically targeting endothelium in early stages of inflammation[24] and a new system for magnetic hyperthermia.[25]

In the frame of this work, we have successfully modified the surface of SPION/CCh with anti-N-cadherin antibodies and studied in detail their physicochemical properties, cytotoxicity, as well as their interaction with PC-3, DU 145, and LNCaP human prostate cancer cell lines. PC-3 cell line is derived from bone metastasis. It does not express prostate-specific antigen (PSA) and is androgen-independent. It shows highly aggressive behaviour and has the mesenchymal, migratory phenotype typical for the cells that underwent EMT. PC-3 cells also show lower E-cadherin and higher N-cadherin expression compared to other prostate cancer cell lines.[26] The DU 145 cell line was derived from a central nervous system metastasis of primary prostate adenocarcinoma origin. DU 145 are not hormone-sensitive and do not express PSA, but they do express androgen receptor. Relative deficiency of transcription factors associated with methylation is responsible for the lack of AR promoter function in most of AR-negative cell lines. Mutations in the AR gene are present in the cells that express the AR but are androgen independent.[27] DU 145 cells show moderate metastatic potential compared to PC-3 cell line, are characterized by epithelial phenotype, and have a much lower N-cadherin expression than PC-3. LNCaP cells are androgen-sensitive human prostate adenocarcinoma cells derived from the left supraclavicular lymph node metastasis. They are adherent epithelial cells, which have low metastatic potential. LNCaP, DU 145 and PC-3 were chosen because they are among the most commonly used prostate cancer cell lines, and they represent different stages of EMT, showing increasingly metastatic character and different levels of N-cadherin expression. The specificity of the antibody toward N-cadherin expressed in prostate cancer cells was studied using AFM, while the interaction of nanoparticles with the antibody was followed by flow cytometry. Finally, the preliminary experiments were performed to evaluate the possibility of applying the proposed nanoparticulate system in the magnetic capture of CTC. The number of cells captured after different incubation times was also determined to verify the possibility of CTC capture in the flow.

Materials and Methods
Materials
Chitosan (Ch, low molecular weight, catalogue no. 448869, Sigma-Aldrich, Poznań, Poland), glycidyltrimethylammonium chloride (GTMAC, ≥90%, catalogue no. 50053, Sigma-Aldrich, Warsaw, Poland), iron (II) chloride tetrahydrate (puriss. p.a., ≥98.5%, catalogue no. 44939, Sigma-Aldrich, Poznań, Poland), iron (III) chloride hexahydrate (puriss. p.a., ≥98.5%, catalogue no. 31232-M, Sigma-Aldrich, Poznań, Poland), p-toluene-sulfonyl chloride (tosyl chloride, TsCl, ReagentPlus®, ≥99%, catalogue no. 240877, Sigma-Aldrich, Poznań, Poland), 1,10-phenanthroline monohydrate (p.a., catalogue no. 413000221, POCH S.A.), polyethylenimine branched (PEI, average Mw ~25,000 by LS, Sigma-Aldrich, Poznań, catalogue no. 408727), t-octylphenoxypolyethoxyethanol (Triton™ X-100, for molecular biology, catalogue no. T8787, Sigma-Aldrich, Poznań, Poland), phosphate-buffered saline (PBS, tablet, catalogue no. P4417, Sigma-Aldrich, Poznań, Poland), ethylenediaminetetraacetic acid (EDTA, ACS reagent, 99.4–100.6%, powder, catalogue no. E9884, Sigma-Aldrich, Poznań, Poland), bovine serum albumin (BSA, BioReagent, suitable for cell culture, catalogue no. A9418, Sigma-Aldrich, Poznań, Poland), fetal bovine serum (FBS, qualified, heat inactivated, catalogue no. 10500064, Gibco, Thermo Fisher Scientific, Warsaw, Poland), (hydroxymethyl)aminomethane (Tris; Sigma Aldrich, Poznań, catalogue no. GE17-1321-01), sodium dodecyl sulfate (SDS; Sigma Aldrich, Poznań catalogue no. GE17-1313-01), β-mercaptoethanol (Sigma Aldrich, Poznań, catalogue no. 444203), glycerol (for molecular biology, ≥99.0%, Sigma Aldrich, Poznań, catalogue no. G5516), Tween® 20 (viscous liquid, Sigma Aldrich, Poznań, catalogue no. P1379), fluorescein isothiocyanate (FITC, BioReagent, ≥90%, catalogue no. 46950, Sigma-Aldrich, Poznań, Poland), Human/Mouse/Rat N-Cadherin Antibody (polyclonal sheep IgG, catalogue no. AF6426, R&D Systems), Donkey Anti-Sheep IgG NorthernLights™ NL557-conjugated Antibody (polyclonal donkey IgG, catalogue no. NL010, R&D Systems, Bio-Techne, Warsaw, Poland), Anti-Sheep IgG HRP-conjugated (R&D Systems, catalogue no. XDP 1421031), Anti-E-cadherin (Cell Signaling Technology, catalogue no. 3195S), β-actin (Cell Signaling Technologies, catalogue no. 4970S), Anti-rabbit IgG HRP-linked (Cell Signaling Technology, catalogue no. 7074), PC-3 cell line (ATCC®, catalogue no. CRL-1435, LGC Standards, Łomianki, Poland), DU 145 cell line (ATCC®, catalogue no. HTB-81, LGC Standards, Łomianki, Poland), LNCaP clone FGC cell line (ATCC®, catalogue no. CRL-1740, LGC Standards, Łomianki, Poland), RPMI 1640 culture medium (Gibco, catalogue no. 21875034, ThermoFisher Scientific, Warsaw, Poland), Qubit Protein Assay Kit (Thermo Fisher Scientific, catalogue no.

Q33211), 3-(4,5-dimethylthiazol-2-yl)-2,5-diphenyltetra-zolium bromide (MTT, powder, BioReagent, ≥97.5% (HPLC), catalogue no. M5655, Sigma-Aldrich, Poznań, Poland), Resazurin sodium salt (Alamar Blue, powder, BioReagent, catalogue no. R7017, Sigma-Aldrich, Poznań, Poland), 4′,6-diamidino-2-phenylindole (DAPI, for nucleic acid staining, catalogue no. D9542, Sigma-Aldrich, Poznań, Poland), were all used as received.

Synthesis of SPION/CCh/N-Cad

CCh was prepared according to the previously developed protocol.[21] The surface of SPION/CCh was further modified by introducing toluenesulfonyl (tosyl, Ts) groups, as described earlier, resulting in SPION/CCh/Ts system.[24] Antibody was dissolved in sterile PBS at a concentration of 0.2 mg/mL. Two milliliters of SPION/CCh/Ts were sonicated for 5 minutes. About 0.54 g of ammonium sulfate in 1.2 mL of filtered borate buffer (pH = 9.5) was added, followed by 50 µL of N-cadherin antibody solution (0.2 mg/mL) in sterile phosphate-buffered saline (PBS). The mixture was incubated at 37 °C for 24 hours with steady agitation (100 rpm). The suspension was centrifuged three times (20 minutes, 10,000 rpm, 25 °C), each time the supernatant was exchanged with fresh borate buffer. The obtained SPION/CCh/N-cad nanoparticles were suspended in borate buffer and stored in a refrigerator.

Characterization Methods

The average size and zeta potential of SPION/CCh/N-cad were measured using Zetasizer Nano ZS (Malvern Instrument Ltd., A.P. Instruments, Warsaw, Poland). Measurements were performed in the deionized water (pH=7, temperature: 25°C, viscosity: 0.8872, Smoluchowski Model: F(κα) value: 1.50). The data were recorded and analyzed using Malvern Zetasizer Nano software v.3.30. Fluorescence spectra were obtained using SLM Aminco 8100 spectrofluorometer (SLM, Rochester, NY) in the quartz cuvette (1 cm optical path) at room temperature. The data were recorded and analyzed using Olis SpectralWorks software. Fourier-Transform Infra-Red (FTIR) spectrum of nanoparticles was recorded using Nicolet iS10 FTIR spectrometer with an Attenuated Total Reflectance (ATR) attachment (Thermo Fisher Scientific, Warsaw, Poland). The data were recorded and analyzed using OMNIC FTIR software. For AFM visualization of the SPION systems, the silicon substrates were pre-conditioned by cleaning with ethanol, and Ultra-Violet

Ozone Cleaner followed by spin-coating with a thin layer of poly(ethyleneimine) (1 mg/mL aqueous solution) to facilitate electrostatic attachment of nanoparticles. SPION/CCh/N-cad or SPION/CCh/Ts were then introduced by deep-coating (10 minutes, sonication with 5 seconds pulses). All results were visualized using Origin Pro 2021.

Biological Studies
Cell Culture Conditions and Cytotoxicity Measurements

Cell culture conditions and cytotoxicity measurements using MTT and Alamar Blue assays are described in detail in the Supplementary Materials.

The level of N-cadherin and E-cadherin for all three cell lines used in our study was verified experimentally, and the results are also presented in Figure S6. The obtained results have confirmed that the level of N-cadherin is the highest for the PC-3 cells, lower for DU 145 and no N-cadherin was observed for LNCaP cell line. For E-cadherin, the tendency was reversed.

Microscopic Imaging of Cell–Nanoparticle Interaction

PC-3 cells were seeded on glass coverslips placed in a 6-well cell culture plate at 950,000 cells/well and incubated for 24 hours until a monolayer of cells was obtained. Co-cultures of cells: PC-3 and DU 145 (cell number ratio 1:1), PC-3 and LNCaP (cell number ratio 1:4) were obtained by simultaneous seeding of cell mixtures on glass coverslips and incubated until a monolayer of cells was observed. Cells in all cultures were then fixed with 4% formaldehyde (20 minutes at room temperature), and permeabilized with 0.2% Triton[TM] X-100 solution (5 minutes at 4 °C). The glass coverslips with fixed cells were then incubated with SPION/CCh/N-cad in the amount corresponding to the anti-N-cadherin antibody concentration of 10 µg/mL or with N-cadherin antibody (10 µg/mL) for 1 hour. Next, the samples were washed with PBS and incubated with secondary antibody labelled with a fluorescent probe (Northern Lights NL577®) for 1 hour. Cell nuclei were stained with DAPI solution. Obtained samples were visualized using an inverted Nikon Ti-E microscope (Precoptic, Warsaw, Poland) equipped with the Nikon A1 confocal system, 405 and 488 nm lasers, two objectives: 40x and 100x oil; and fluorescent filter blocks: DAPI, FITC. The images were

collected and analyzed using NIS-Elements confocal software.

Flow Cytometry Measurements

PC-3, DU 145 and LNCaP cell lines were cultured in supplemented RPMI 1640 medium containing 10% (v/v) of FBS under culture conditions. Cells were detached from a dish surface using 0.02 M EDTA solution. Cell suspensions were centrifuged (6 minutes, 1500 rpm, 4°C), washed with 2% BSA in PBS solution, counted using a cell counter (Invitrogen, Thermo Fisher Scientific, Warsaw, Poland), and suspended in fresh PBS (1,000,000 cells/mL). Samples of PC-3 cells, DU 145 cells and LNCaP cells were prepared and incubated with fluorescently labeled SPION/CCh/N-cad (the number of added nanoparticles corresponded to the anti-N-cadherin antibody concentration of 2.5 µg/mL) for 1 hour at 4 °C.

To evaluate the kinetics of SPION/CCh/N-cad attachment to PC-3 cells, 10,000 cells were suspended in 0.5 mL PBS and incubated with the same SPION/CCh/N-cad concentration (corresponding to the anti-N-cadherin antibody concentration of 2.5 µg/mL) for 1 minute, 5 minutes, 10 minutes, 20 minutes, 30 minutes, and 1 hour. After the respective time, the samples were centrifuged, washed with 2% BSA in PBS solution and measured using BD™ LSR II flow cytometer (BD Biosciences, Warsaw, Poland). Forward and side scatter signals were used to gate for morphologically normal cells. The data obtained were recorded using BDFACSDiva™ v9.0 and analyzed using FlowJo™ v10.8 program to determine the percentage and mean fluorescence intensity of positive cells.

AFM Studies of the SPION Systems and of the Antibody Specificity

AFM images of SPION systems were obtained in air using Dimension Icon AFM (Bruker, Santa Barbara, CA, USA). AFM was operating in the PeakForce QNM® mode (Peak Force frequency 1 kHz). ScanAsyst-AIR probes with a nominal spring constant of 0.4 N/m and nominal tip radius of 2 nm were used for topography measurements. AFM images were captured with resolution of 384×384 pixels. The SPION samples were diluted to ca. 0.1 mg/mL and spin-coated on the surface of PEI-coated silicone substrate.

The antibody specificity toward N-cadherin on the surface of PC-3 and DU 145 cells was also investigated with AFM. PC-3 and DU 145 cells were seeded on glass coverslips placed in a 6-well cell culture plate and incubated for 48 hours under culture conditions. Each coverslip was next placed in the liquid cell and covered with a fresh cell culture medium. Samples in which N-cadherin was blocked (control) were prepared analogously, but directly before the measurement the cells were incubated for 30 minutes in 0.2 mM EDTA solution in a culture medium. Meanwhile, the MLTC B cantilever (0.02 N/m, 8.56 Hz, Bruker) was modified by attaching an anti-N-cadherin antibody. The cantilever was first surface-modified using APTES from the gas phase, then surface activated with 0.5% glutaraldehyde in PBS, and incubated in the anti-N-cadherin antibody solution (0.01 µg/mL in PBS) for 1 hour at room temperature.[28] Adhesion measurements were performed using AFM (model XE120, Park Systems, Korea) operating in the semi-contact mode; the force limit was set to 1 nN, the Z Highest was +9 µm and the Z Lowest was −9 µm. The data were recorded using XE Data Acquisition Program. For each cell line, the unbinding force experiments were conducted for 5 different retraction speeds, ie, 2, 4, 6, 8, 10 µm/s. For each speed, 3 series of measurements, each done for 10 cells, were performed (in total 150 cells were measured for one cell line). Each cell was mapped, ie, 25 force–distance curves were recorded over a 25 µm² area. Analogous measurements were carried out for cells in which N-cadherin was blocked. All the obtained force–distance curves were analyzed using FORCE v.11.0 software and visualized using Origin Pro 2021.

Magnetic Capture of PC-3 Cells

PC-3 and DU 145 cell lines were cultured in supplemented RPMI 1640 medium containing 10% (v/v) of FBS under culture conditions. Cells were detached using 0.02 M EDTA solution. Cell suspensions were centrifuged (6 minutes, 1500 rpm, 4 °C), washed with 2% BSA in PBS solution and counted using a cell counter. Cells were then suspended in fresh PBS (10,000 cells/mL) and incubated with SPION/CCh/N-cad (the number of nanoparticles corresponded with anti-N-cadherin antibody concentration of 2.5 µg/mL) for 1 hour at 37 °C. After that, samples were centrifuged and washed with PBS. Cell pellets were re-suspended with 1 mL of fresh PBS and placed in a specially designed cuvette. A neodymium magnet was then placed at the side of the cuvette. The system was left for 10 minutes; then the shutter was closed, separating the liquid from the narrow part of the cuvette adjacent to the magnet. The solution was collected from the other part of the cuvette and, finally, the suspension remaining in the narrow part, close to the magnet, was

retrieved. The experiment was repeated three times. The magnetically captured cell-SPION systems were then counted using an optical microscope.

Results

Synthesis of the SPION/CCh/N-Cad

SPION stabilized by CCh were prepared according to the protocols developed previously by Zapotoczny et al.[21] The resulting SPION/CCh nanoparticles were then surface modified in order to target them to N-cadherin present on the surface of the cancer cells. The schematic representation of the reaction steps and nanoparticles interaction with cancer cells is shown in Figure 1. First, active tosyl groups were introduced on SPION/CCh surface. To achieve that, the hydroxyl groups of CCh on the nanoparticles' surface were reacted with TsCl. The reaction was performed in pyridine, which was used as both a solvent and a catalyst.[24] The presence of Ts groups on the surface of resulting SPION/CCh/Ts nanoparticles was confirmed using ATR-FTIR spectroscopy, as described in detail in Figure S1. The obtained SPION/CCh/Ts were then decorated with anti-N-cadherin antibodies. Due to the presence of active tosyl groups, the conjugation reaction could be conducted in aqueous

conditions (pH = 9.5, 37 °C). The amount of the attached antibody in the resulting SPION/CCh/N-cad sample was estimated by immunostaining with secondary, fluorescent antibody, while the concentration of iron in the same sample was determined based on colorimetric assay using 1,10-phenanthroline, after all Fe^{3+} ions were reduced to Fe^{2+} with ascorbic acid (Figure S2). The calculated content of the anti-N-cadherin antibody on the surface of SPION/CCh/N-cad was estimated as 0.024 µg/µg Fe. In the optimized conditions around 44% of the antibody was successfully attached to the nanoparticles.

Physicochemical Properties of SPION/CCh/Ts and SPION/CCh/N-Cad

The average size of the nanoparticles, their polydispersity index (PDI) and colloidal stability, evaluated based on their zeta potential, were determined using DLS/ELS technique. Table 1 summarizes the results obtained for SPION/CCh/Ts and SPION/CCh/N-cad systems. Comparing the iron concentration in both suspensions indicates that the attachment reaction was conducted without a significant loss of the nanoparticles.
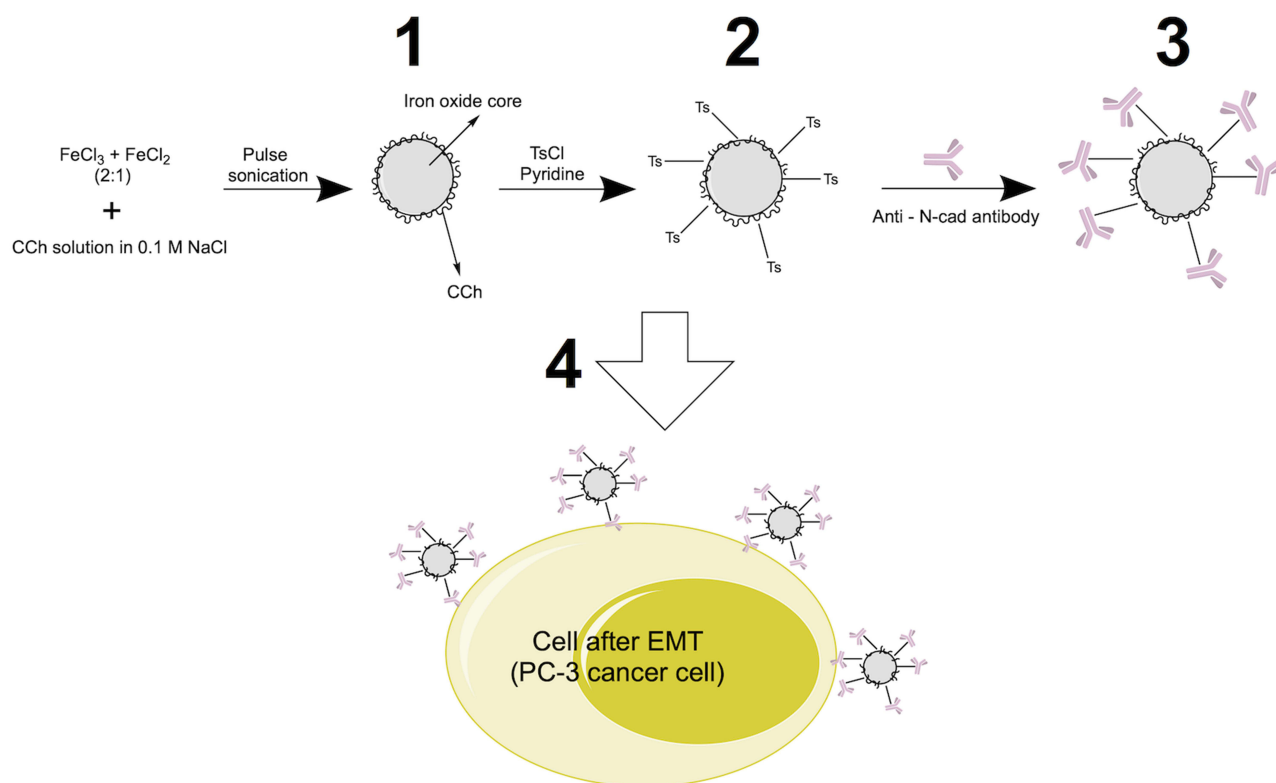

Figure 1 Schematic representation of the synthesis of the SPION/CCh/N-cad system (1–3) and the interaction of this system with cancer cells after EMT (PC-3 cells) characterized by high N-cadherin expression (4).

Table 1 Physicochemical Properties of the SPION/CCh/Ts and SPION/CCh/N-Cad Suspensions

Name of the Sample	The Average Size [nm]	PDI	Zeta Potential [mV]	Iron Concentration [μg/mL]
SPION/CCh/Ts	143 ± 1	0.309 ± 0.022	+ (41.5 ± 0.8)	194 ± 20
SPION/CCh/N-cad	223 ± 4	0.211 ± 0.019	- (45.5 ± 1.69)	180 ± 32

To get a deeper insight into the morphology and aggregation phenomena in SPION/CCh/Ts and SPION/CCh/N-cad samples, they were visualized using AFM. The images obtained for dry samples are presented in Figure 2. Tosylated SPION (images A and C) had a spherical shape and only a moderate tendency to aggregate, with an average size in the range of 20–25 nm. The SPION/CCh/N-cad particles were also spherical, somewhat bigger (ca 30 nm), and had a significantly higher tendency to aggregate (images B and D). The aggregates in the range of 150–500 nm were observed, forming larger structures resembling chains of beads. No individual particles of smaller size were observed. The applied PeakForce QNM mode enabled simultaneous capturing of adhesion maps (images E and F), which provided an insight in tip–sample interactions. The regions showing lower adhesion were assigned to the modified SPION while those with higher adhesion to PEI-coated silicon substrate. In aqueous suspensions, the SPION/CCh/Ts and SPION/CCh/N-cad particles had an average size of 143 and 223 nm, respectively. Zeta potential values confirmed their colloidal stability. Differences in the values obtained by AFM and DLS measurements can be explained considering that AFM measurements were performed for the dry samples, where no hydrating layer is present, nor is the polymeric coating expanded.

The excellent magnetic properties of the nanoparticles were confirmed based on Mössbauer spectroscopy and magnetometry (Figures S3–S5).

Biological Studies

Cytotoxicity of SPION/CCh/N-Cad Nanoparticles

One of the most important parameters determining the applicability of a system in biological research is its cytotoxicity.[29] In order to test whether SPION/CCh/N-cad have a toxic effect on the prostate cancer cells, the MTT and Alamar Blue tests were performed. The range of concentrations of the nanoparticles studied was adjusted to the needs of the further experiments, particularly to the minimal antibody concentrations required for the reliable flow cytometry measurements. The obtained results are summarized in Figure 3.

While the observed cell viabilities according to the Alamar Blue test are higher, the observed tendencies are identical – the viability of PC-3 slightly decreased with SPION/CCh/N-cad concentration, but even for the highest concentration it remained relatively high, above 80%.

AFM Studies of the Interaction of Antibodies with Cells

The interactions between the anti-N-cadherin antibody used to modify our nanoparticles and two prostate cancer cell lines, PC-3 and DU 145, differing in N-cadherin expression, were performed with AFM, as this technique is well suited to study interactions in biological systems[30] and provides a single-molecule accuracy. As a first parameter, the unbinding probability was determined. Its value describes the abundance of N-cadherin on the cell surface and may be roughly linked with the N-cadherin expression. The unbinding probability is defined as the ratio of unbinding events to the total number of force curves recorded during the experiment. In our study, 3750 curves were recorded for each cell type. A total of 2223 unbinding events were obtained for PC-3 cells and 1270 were obtained for DU 145 cells, which constituted 59% and 34% of all recorded force curves, respectively. To confirm the specificity of the observed interactions, the experiments in which N-cadherin was blocked with the 0.2 mM EDTA were conducted (Figure 4A and B). The addition of EDTA decreased the number of unbinding events. The unbinding probability dropped by 20% (1414 observed unbinding events) and 10% (847 events) for PC-3 and DU 145 cells, respectively. The retraction part of the recorded force curves was analyzed to calculate the unbinding force characteristic for the antibody-N-cadherin interaction (Figure 4C and D).

The force value was calculated as a force needed to detach the antibody-modified tip from the cell surface. The obtained values of the unbinding force were further plotted as a function of the loading rate (calculated by multiplying the retraction velocity by the effective spring constant originating from the convolution of cantilever and molecular complex). The loading rate describes how fast the force changes in time during the complex rupture. The relations of the unbinding
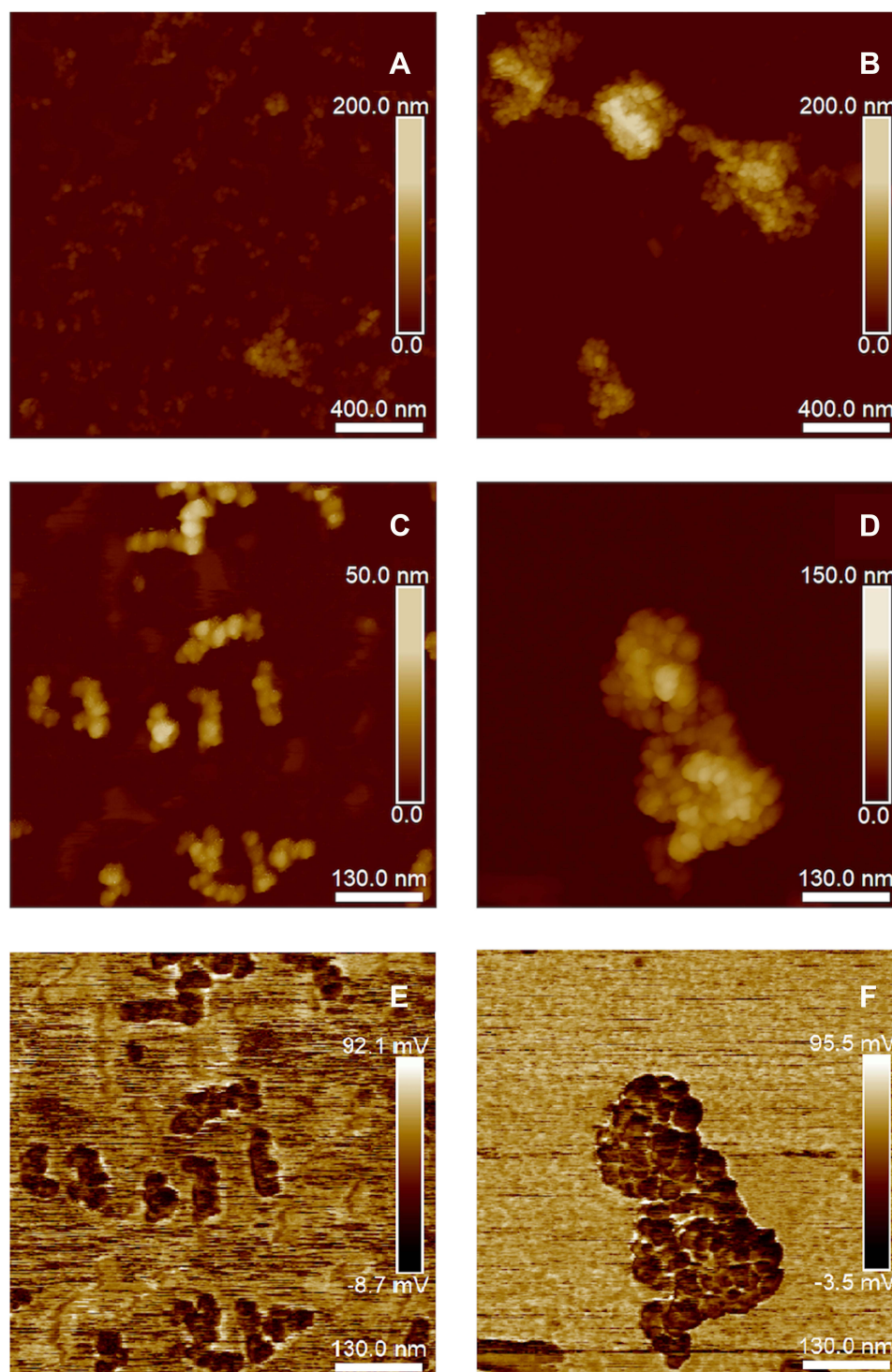
Figure 2 AMF images of SPION/CCH/Ts (**A** and **C**) and SPION/CCh/N-cad (**B** and **D**); adhesion maps for SPION/CCH/Ts (**E**) and SPION/CCh/N-cad (**F**).

force obtained for N-cadherin-antibody interaction occurring on PC-3 and DU 145 cells are presented in Figure 5.

Measurements of the unbinding force for N-cadherin-antibody complexes present on a PC-3 and DU 145 cell surface were performed within the same retraction speed range (2–10 µm/s). The corresponding range of the loading rate was from 320 to 1840 pN/s in the case of measurements conducted on a surface of PC-3 cells and from 92 to 2370 pN/s for measurements carried out on the surface DU 145 cells. The range of the unbinding forces
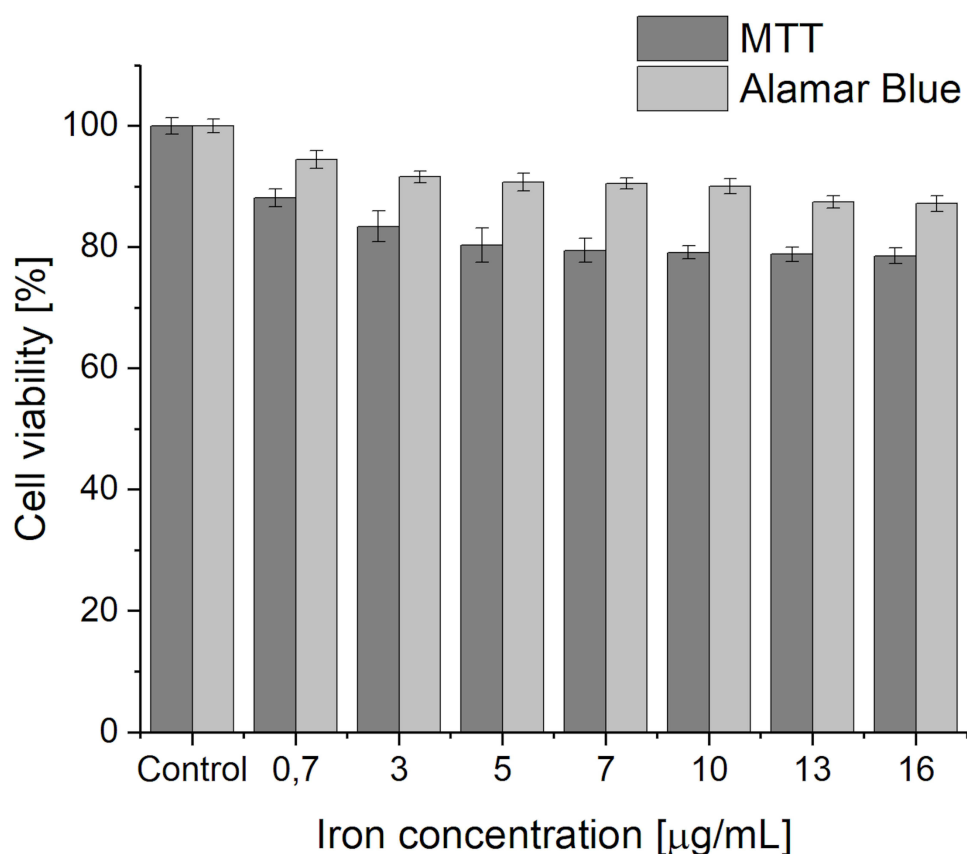
Figure 3 The results of MTT and Alamar Blue viability assays for the PC-3 cells incubated with various concentrations of SPION/CCh/N-cad.

calculated for these limits was from 26.8 ± 0.9 to 41.5 ± 1.0 pN for PC-3 and from 40.9 ± 0.9 to 52.1 ± 1.6 pN for DU 145. The loading rate dependence of the anti-N-cadherin/N-cadherin interaction demonstrates that the measured interaction has a specific character.[31]

Interaction of SPION/CCh/N-Cad Nanoparticles with Cancer Cells

The studies on the interaction of SPION/CCh/N-cad with three different cancer cell lines differing in the amount of N-cadherin present on their surface were performed using flow cytometry. The polymer coating of the nanoparticles was labeled with FITC before the anti-N-cadherin antibody was attached. The obtained fluorescent F-SPION/CCh/N-cad allowed us to gain an unambiguous information about their interactions with cells while avoiding using a fluorescently labeled secondary antibody, and thus its non-specific interactions with cells. The obtained results are summarized in Figure 6.

The histograms show the cell counts for the different cell types pre-incubated with SPION/CCh/N-cad (blue-shaded) compared to the untreated controls cells (red-shaded). The

vertical black line cuts off the autofluorescence signal from untreated cells, while the range horizontally marked as "fluorescence" shows the histogram section representing the fluorescence observed from the cancer cells with attached nanoparticles. The percentages of positive cells and the MFI (Mean Fluorescence Intensity) values are also given. The analysis of histograms shows a significant signal from the nanoparticles attached to the PC-3 cells (49.4%), confirming the effective binding of these cells. The nanoparticles have attached to some of the DU 145 cells (23.7%), but the effect was clearly weaker than in the case of PC-3 cells. The results obtained from the cytometry are correlated with the unbinding probability values obtained from AFM experiments (59% and 34% of unbinding events registered for PC-3 and DU 145 cells, respectively). The percentage of DU 145 cells with attached nanoparticles was about two times, and the MFI value for these cells was about three times lower than for PC-3 cells. In the case of LNCaP cells, the fluorescence of cells incubated with SPION/CCh/N-cad does not extend significantly beyond the autofluorescence area (1.64%). LNCaP cells easily aggregate, which may affect the non-specific attachment of nanoparticles, and this
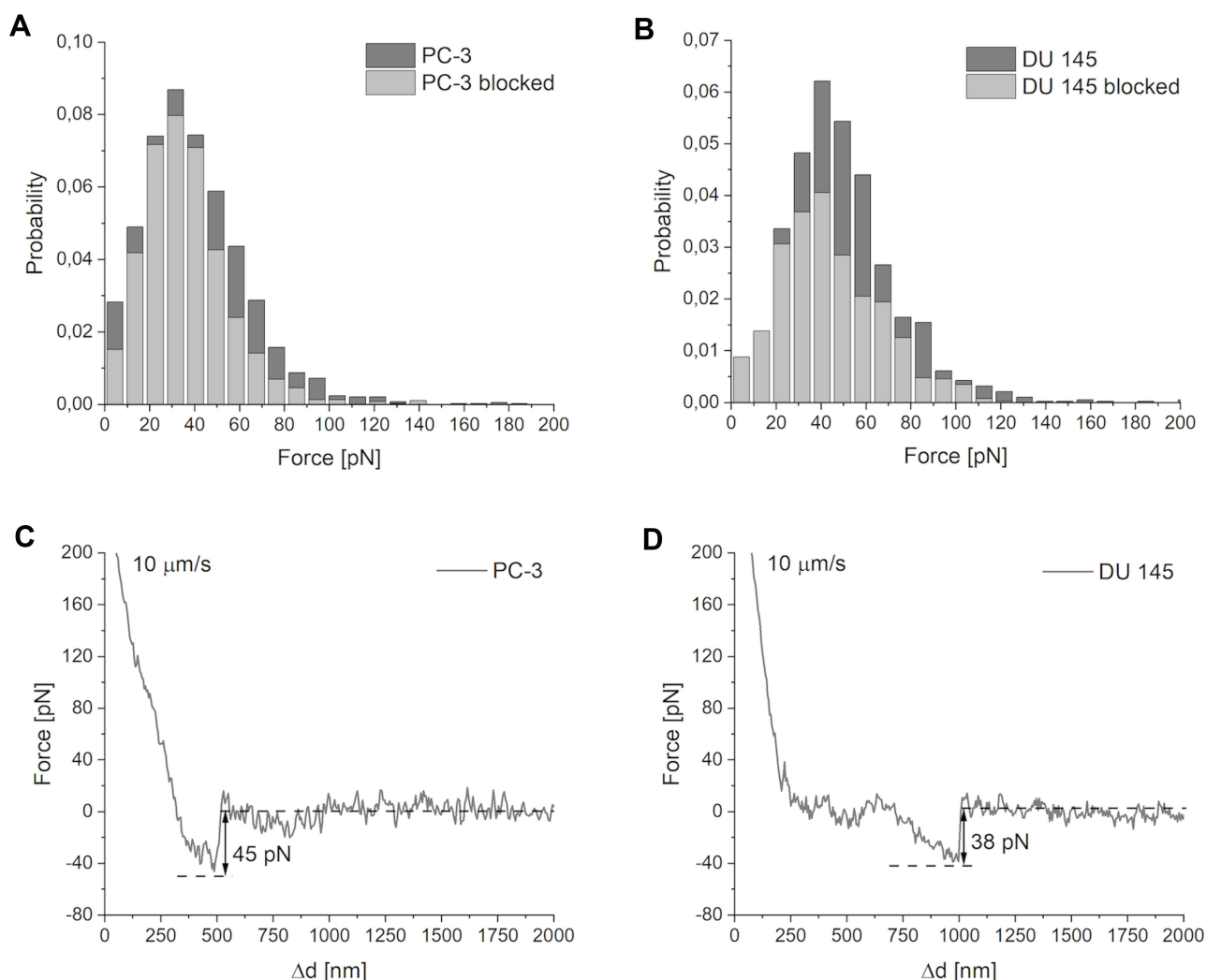
Figure 4 Effect of N-cadherin inhibition on the probability of unbinding events for PC-3 (**A**) and DU 145 (**B**) cell lines and exemplary force curves showing a single unbinding of PC-3 (**C**) and DU 145 (**D**) for a loading rate of 6330 and 10,700 pN/s, respectively.

would explain the small number of cells in the SPION/CCh/N-cad fluorescence range.

The use of a confocal microscope allowed us to visualize the antibody distribution itself and the SPION/CCh/N-cad nanoparticles in the monoculture of PC-3 cells (Figure 7A and B) and in the co-cultures of different cancer cell lines (Figure 7C and D). For visualization, the N-cadherin antibody and SPION/CCh/N-cad were immunostained with fluorescent secondary antibody labelled with NorthernLights™ NL557 chromophore (red fluorescence). Cell nuclei were stained with DAPI to obtain better images.

Both antibodies and nanoparticles with bound antibody bind efficiently to the surface of PC-3 cells. Figure 7C clearly shows the places where SPION/CCh/N-cad fluorescence is not observed or is very weak. Instead, in the same places, the well-visible nuclei of LNCaP cells can be

observed, confirming that our particles attach selectively to N-cadherin on the surface of PC-3 cells. In Figure 7D, only the nuclei of DU 145 cells are visible in the focus of the image. This is because these cells have grown up on cells from the PC-3 line, which were therefore out of the focal distance, below the layer of DU 145 cells.

Magnetic Capture of PC-3 Cells

Magnetic capture of PC-3 and DU 145 cells was performed under quasi-stationary conditions, and the course of the experiment is schematically presented in Figure 8. The cells were first incubated with SPION/CCh/N-cad nanoparticles. The suspension was then placed in the especially designed, 3D printing made cuvette (1) and a neodymium magnet was applied to the side of the cuvette (2). After the respective time, the shutter inside the
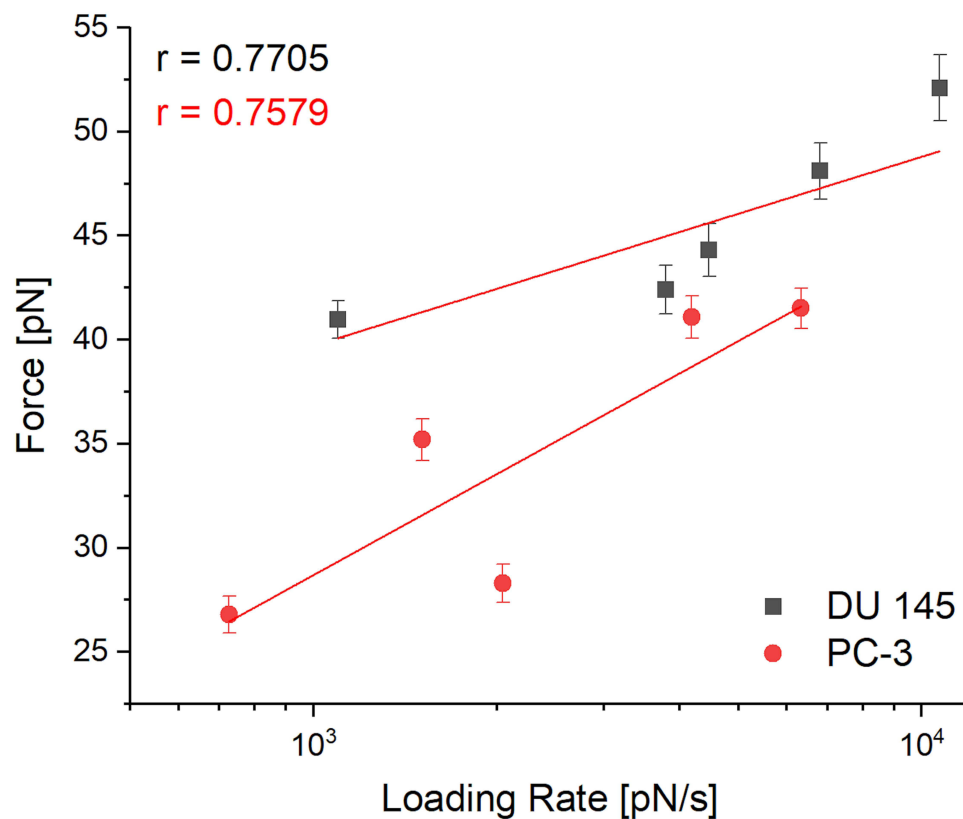
Figure 5 The unbinding force for N-cadherin-antibody complexes plotted as a function of the logarithm of the loading rate. Each point represents the mean value ± standard error (sem). The N-cadherin-antibody complex on the surface of PC-3 and DU 145 cells was studied.
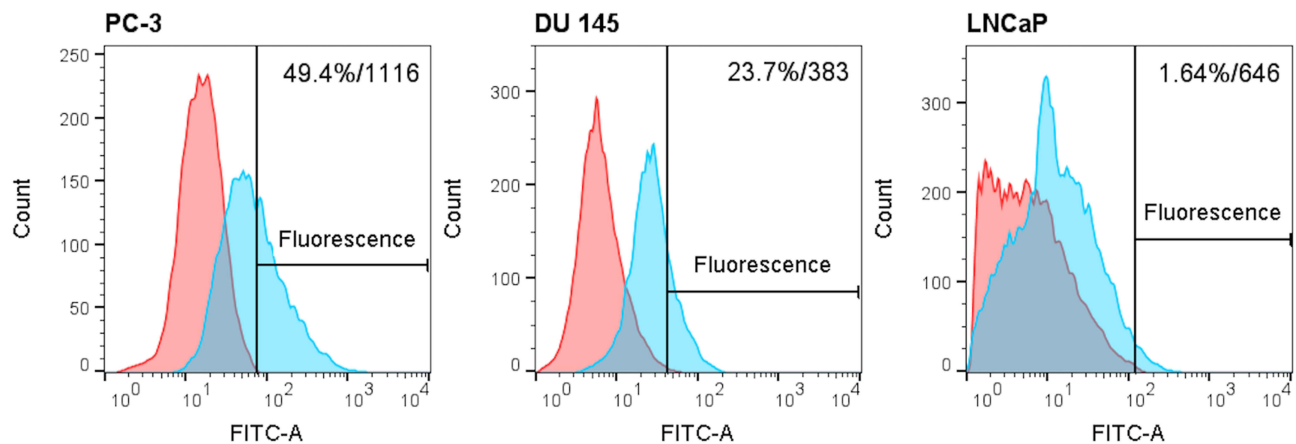

Figure 6 Flow cytometry histograms for PC-3, DU 145 and LNCaP cell lines incubated for 1 h with F-SPION/CCh/N-cad (blue-shaded) compared to untreated control cells (red-shaded). The percentages of the cells with attached F-SPION/CCh/N-cad and the observed MFI (Mean Fluorescence Intensity) values are given in histograms.

cuvette was closed, dividing it into two compartments (3). The suspensions of cells from both compartments were then moved to the vials and analyzed (4).

Magnetic capture of PC-3 cells was achieved with high efficiency; more than 80% of the cells were effectively captured in the compartment next to the magnet. The mean value of the number of captured cells obtained from three

independent experiments was 8126 (total number of cells: 10,000). In the DU 145 cell line only 3748 cells out of 10,000 were captured, which may be explained by the weaker binding of nanoparticles to the cell surface due to the lower expression of N-cadherin.

For the sake of the possible future application in a flow system, the influence of the incubation time of PC-3 cells
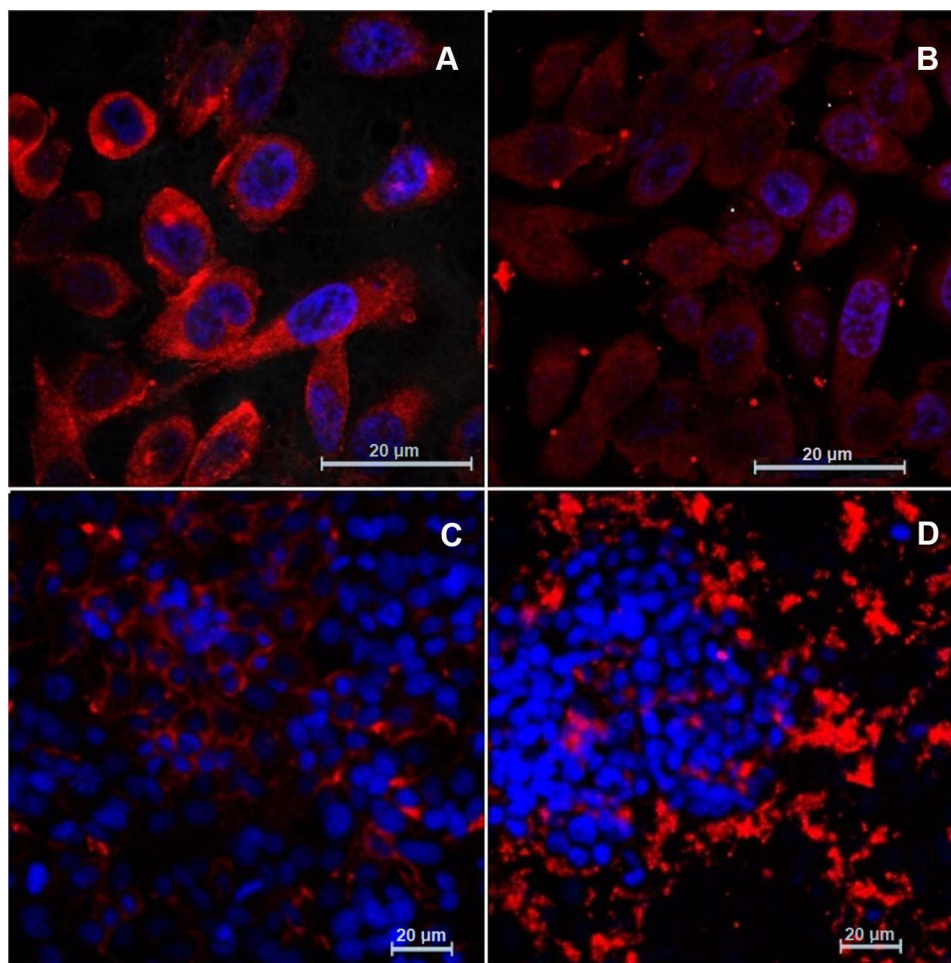
Figure 7 Images of PC-3 cells incubated with: A – N-cadherin antibody; B – SPION/CCh/N-cad, and images of the co-cultures incubated with SPION/CCh/N-cad: C - PC-3 and LNCaP cells; D - PC-3 and DU 145 cells. Scale bar size is 20 µm.

with SPION/CCh/N-cad on the capture efficiency was also determined. The results obtained from the cytometric measurements are shown in Figure 9.

The vertical line in the graph marks the boundary between autofluorescence and the fluorescence observed from the nanoparticles bound to the cells. The obtained results show that SPION/CCh/N-cad attach effectively to the cells after just 1 minute of incubation and the effect up to 30 minutes of incubation is not improved. After 1 hour of incubation, the number of attached cells increases by 50%.

Discussion

While EMT was clearly shown to facilitate metastasis, and N-cadherin expression can be undoubtedly related to aggressive tumors, to the best of our knowledge, neither a SPION-based system actively targeting N-cadherin in cancer cells was reported yet nor was such a system used

for the capture of cancer cells. Therefore, we have modified the previously obtained and characterized SPION/CCh particles[21] with anti-N-cadherin antibody in order to target actively cancer cells that underwent epithelial–mesenchymal transition (EMT). The tosylate treatment procedure was exploited.[32] The SPION/CCh surface was first modified with tosyl groups to obtain SPION/CCh/Ts, and then the anti-N-cadherin antibody was attached, resulting in SPION/CCh/N-cad system. The physicochemical properties of the nanoparticles were then investigated. The results presented in Table 1 show that SPION/CCh/Ts suspensions are colloidally stable, as the magnitude of zeta potential is significantly above 30 mV. Antibody attachment resulted in the change of the surface charge from positive to negative and reduced its absolute value to about 20 mV. The aggregation process was indeed detected for more concentrated SPION/CCh/N-cad suspensions. This tendency was also observed with
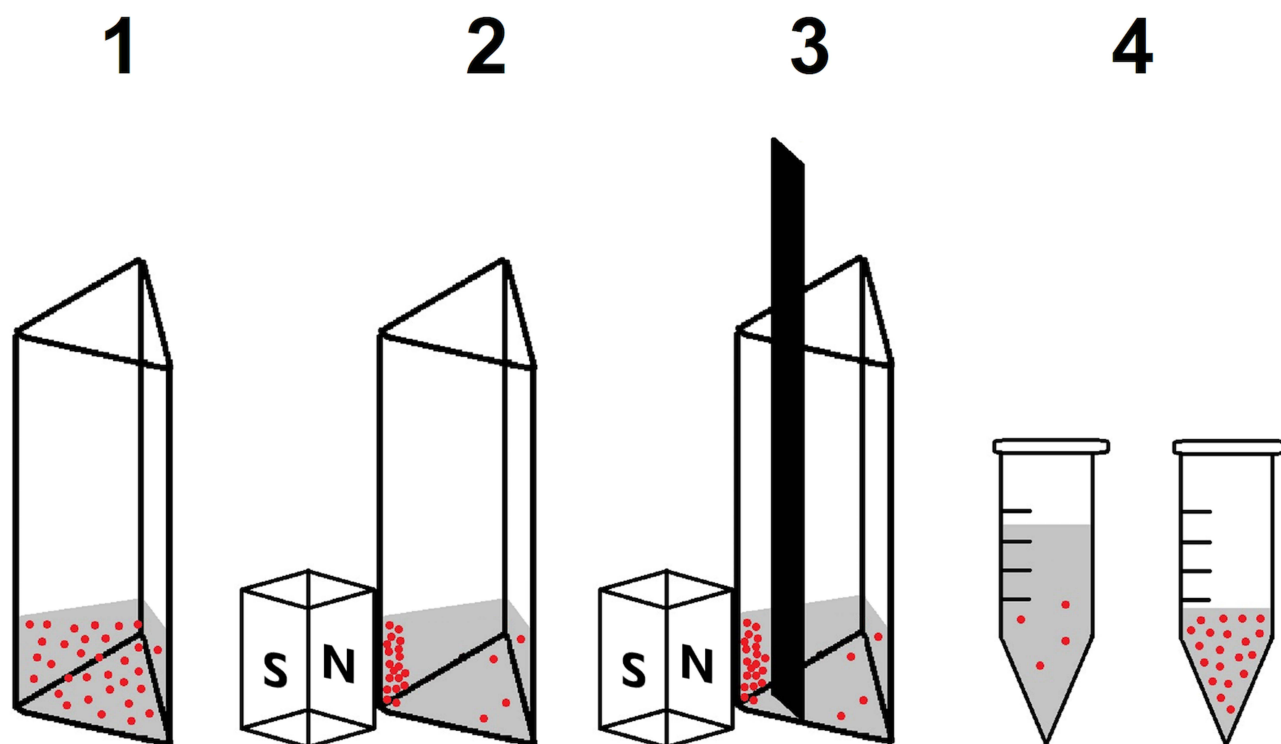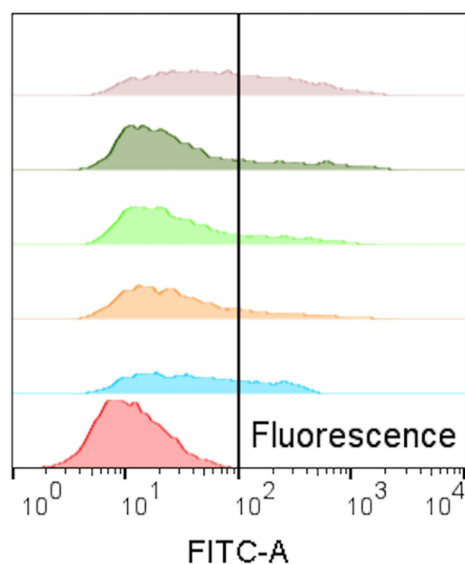
Figure 8 Scheme of quasi-stationary cell capture: 1 - introducing the cell suspension into the cuvette, 2 - capturing cells using a neodymium magnet, 3 - separating the captured cells by closing the shutter, 4 - collecting the solution separated by the shutter and the suspension of the captured cells.

Sample Name	MFI	% of Fluorescent Cells
1 h	2077	39.4
30 min	1985	20.4
10 min	2124	18.4
5 min	2202	17.8
1 min	2237	25.5
Control	2371	0

Figure 9 Flow cytometry histograms for PC-3 cell line incubated with FITC-labelled SPION/CCh/N-cad for different time intervals.

AFM measurements where antibody-modified particles formed clearly visible aggregates of several hundreds of nanometers in size. The nanoparticles, both before and after modification, had regular spherical shapes and sizes in the range of 140 and 220 nm, respectively. Superparamagnetic properties of the synthetized system were confirmed by Mössbauer spectroscopy and magnetometry (see Supplementary Materials). The prepared SPION/CCh material was found to have excellent magnetic properties, as reported elsewhere,[23,24] and the measurements confirmed that its modification had no negative influence on them.

In the next step, we have studied the interactions between the SPION system obtained and cancer cells expressing N-cadherin on their surface. N-cadherin is well known to be abundantly present in PC-3 cells; a low activity of this protein can also be observed in the DU 145 line, the latter being a suitable model of the cancer cells undergoing EMT. We have confirmed it on the cell lines used in this study (Figure S6).

To ensure that the SPION/CCh/N-cad in the concentration used would not result in a significant death rate of PC-3 cells, interfering with further experiments, we have first performed cytotoxicity measurements, applying MTT and Alamar Blue assays. The obtained results showed the same trend, even though the observed values somewhat differed. Cell viability decreased slightly with increasing concentration of nanoparticles, but even for the highest concentration used (16 µg/mL of iron), it was still very high, in the range of 80–90%. Therefore, it was concluded that the SPION/CCh/N-cad system has a negligible toxic effect on the studied cells within the investigated concentration range.

Further on, the specificity of the interaction between the selected anti-N-cadherin antibody and N-cadherin expressing cells was confirmed by AFM studies, in which the antibody was covalently attached to the AFM tip. Flow cytometry measurements, performed using FITC-labelled nanoparticles for three different prostate cancer cell lines differing in N-cadherin expression, revealed that the percentage of DU 145 cells with attached nanoparticles was about two times lower than PC-3 cells. For LNCaP cells, characterized by epithelial phenotype, no visible attachment of SPION/CCh/N-cad was observed. These studies confirmed further that the attachment of the nanoparticles to the cancer cells was N-cadherin specific. Confocal microscopy visualization showed that both antibody and SPION/CCh/N-cad bind to the surface of PC-3 cells (see a well-visible red fluorescence in Figure 7). SPION/CCh/N-cad, as well as a free antibody, were evenly distributed over the entire cell surface. The difference in the observed fluorescence intensity of the images obtained for the free antibody and the SPION/CCh/N-cad system may be explained by a presence of the larger aggregates of nanoparticles (Figure 7B), characterized by a strong fluorescence, which enforced the decrease in the overall excitation intensity. Importantly, large aggregates did not attach to the cell surface.

The preliminary studies on the magnetic capture confirmed that our nanoparticles interact with cancer cells via specific interaction with N-cadherin protein. As DU 145 cells represent the fraction of circulating tumor cells undergoing EMT, it may be concluded that the nanoparticles are more effective in capturing the cells that already underwent a complete phenotype change. Finally, the preliminary flow cytometry studies confirmed that SPION/CCh/N-cad effectively attach to the PC-3 cells already after 1 minute of incubation, and the effect does not increase up to 30 minutes of incubation. After 1 hour, the number of cells with bound nanoparticles increases by 50%. Therefore, it should be possible to use the SPION/CCh/N-cad system for magnetic capture of metastatic cancer cells expressing N-cadherin in the flow conditions, although further optimization of the system is necessary.

Conclusion

The new SPION/CCh/N-cad system was synthetized, and its physicochemical, magnetic, and biological properties studied. It was confirmed that anti-N-cadherin antibody was successfully attached to the surface of previously tosylated SPION. The attached antibody was shown to be selective toward N-cadherin present on the surface of PC-3 and DU 145. The flow cytometry experiments allowed to confirm their selective interaction with N-cadherin on the surface of cancer cells which underwent EMT. Finally, the studies of the magnetic cell capture showed that PC-3 cells were successfully captured. The preliminary flow cytometry studies confirmed that SPION/CCh/N-cad effectively attach to the PC-3 cells already after 1 minute of incubation. As N-cadherin is known to be expressed on the surface of circulating tumor cells, the proposed system can find application in the magnetic capture of such cells, possibly also in the flow conditions.

Acknowledgments

Disclosure

References

1. Dillekås H, Rogers MS, Straume O. Are 90% of deaths from cancer caused by metastases? *Cancer Med*. 2019;8(12):5574–5576. doi:10.1002/cam4.2474
2. Martin TA, Jiang WG. Loss of tight junction barrier function and its role in cancer metastasis. *Biochim Biophys Acta Biomembr*. 2009;1788(4):872–891. doi:10.1016/j.bbamem.2008.11.005
3. Guarino M. Epithelial-mesenchymal transition and tumour invasion. *Int J Biochem Cell Biol*. 2007;39(12):2153–2160. doi:10.1016/j.biocel.2007.07.011
4. Stemmler MP. Cadherins in development and cancer. *Mol Biosyst*. 2008;4(8):835–850. doi:10.1039/b719215k
5. Dulińska J, Bartosz L, Aleksandra G, Dorota L, Tomasz G. Could the kinetin riboside be used to inhibit human prostate cell epithelial – mesenchymal transition? *Med Oncol*. 2020;37(3):1–14. doi:10.1007/s12032-020-1338-1
6. Wheelock MJ, Shintani Y, Maeda M, Fukumoto Y, Johnson KR. Cadherin switching. *J Cell Sci*. 2008;121(6):727–735. doi:10.1242/jcs.000455
7. Hazan RB, Kang L, Whooley BP, Borgen PI. N-cadherin promotes adhesion between invasive breast cancer cells and the stroma. *Cell Commun Adhes*. 1997;4(6):399–411. doi:10.3109/15419069700904457
8. Gravdal K, Halvorsen OJ, Haukaas SA, Akslen LA. A switch from E-cadherin to N-cadherin expression indicates epithelial to mesenchymal transition and is of strong and independent importance for the progress of prostate cancer. *Clin Cancer Res*. 2007;13(23):7003–7011. doi:10.1158/1078-0432.CCR-07-1263
9. Hazan RB, Phillips GR, Qiao RF, Norton L, Aaronson SA. Exogenous expression of N-cadherin in breast cancer cells induces cell migration, invasion, and metastasis. *J Cell Biol*. 2000;148(4):779–790. doi:10.1083/jcb.148.4.779
10. Hotz B, Arndt M, Dullat S, Bhargava S, Buhr HJ, Hotz HG. Epithelial to mesenchymal transition: expression of the regulators snail, slug, and twist in pancreatic cancer. *Clin Cancer Res*. 2007;13(16):4769–4776. doi:10.1158/1078-0432.CCR-06-2926
11. Li G, Satyamoorthy K, Herlyn M. N-cadherin-mediated intercellular interactions promote survival and migration of melanoma cells. *Cancer Res*. 2001;61(9):3819–3825.
12. Ferreira MM, Ramani VC, Jeffrey SS. Circulating tumor cell technologies. *Mol Oncol*. 2016;10(3):374–394. doi:10.1016/j.molonc.2016.01.007
13. Pantel K, Brakenhoff RH, Brandt B. Detection, clinical relevance and specific biological properties of disseminating tumour cells. *Nat Rev Cancer*. 2008;8(5):329–340. doi:10.1038/nrc2375
14. Marrinucci D, Bethel K, Kolatkar A, et al. Fluid biopsy in patients with metastatic prostate, pancreatic and breast cancers. *Phys Biol*. 2012;9(1):016003. doi:10.1088/1478-3975/9/1/016003
15. Mikolajczyk SD, Millar LS, Tsinberg P, et al. Detection of EpCAM-negative and cytokeratin-negative circulating tumor cells in peripheral blood. *J Oncol*. 2011;2011:1–10. doi:10.1155/2011/252361
16. Serrano MJ, Ortega FG, Alvarez-Cubero MJ, et al. EMT and EGFR in CTCs cytokeratin negative non-metastatic breast cancer. *Oncotarget*. 2014;5(17):7486–7497. doi:10.18632/oncotarget.2217
17. Satelli A, Brownlee Z, Mitra A, Meng QH, Li S. Circulating tumor cell enumeration with a combination of epithelial cell adhesion molecule-and cell-surface vimentin-based methods for monitoring breast cancer therapeutic response. *Clin Chem*. 2015;61(1):259–266. doi:10.1373/clinchem.2014.228122
18. Dulińska-Litewka J, Łazarczyk A, Hałubiec P, Szafrański O, Karnas K, Karewicz A. Superparamagnetic iron oxide nanoparticles-current and prospective medical applications. *Materials*. 2019;12(4):617. doi:10.3390/ma12040617
19. Singh AV, Dad Ansari MH, Dayan CB, et al. Multifunctional magnetic hairbot for untethered osteogenesis, ultrasound contrast imaging and drug delivery. *Biomaterials*. 2019;219:119394. doi:10.1016/j.biomaterials.2019.119394
20. Singh AV. Commentary on "Peptide-Conjugated Nanoparticles as Targeted Anti-angiogenesis Therapeutic and Diagnostic in Cancer" by Shaker A. Mousa, Pharmaceutical Research Institute, Albany College of Pharmacy and Health Sciences, Rensselaer, NY 12144, United States. *Curr Med Chem*. 2020;27(17):2927–2928. doi:10.2174/092986732717200604120627
21. Zapotoczny S, Szpak A, Kania G, Skórka T, Tokarz W, Nowakowska M. Stable aqueous dispersion of superparamagnetic iron oxide nanoparticles protected by charged chitosan derivatives. *J Nanoparticle Res*. 2013;15:1. doi:10.1007/s11051-012-1372-9
22. Szpak A, Fiejdasz S, Prendota W, et al. T 1 – t 2 Dual-modal MRI contrast agents based on superparamagnetic iron oxide nanoparticles with surface attached gadolinium complexes. *J Nanoparticle Res*. 2014;16:2678. doi:10.1007/s11051-014-2678-6
23. Strączek T, Fiejdasz S, Rybicki D, et al. Dynamics of superparamagnetic iron oxide nanoparticles with various polymeric coatings. *Materials*. 2019;12:1793. doi:10.3390/ma12111793
24. Kaczyńska A, Guzdek K, Derszniak K, et al. Novel nanostructural contrast for magnetic resonance imaging of endothelial inflammation: targeting SPIONs to vascular endothelium. *RSC Adv*. 2016;6:76. doi:10.1039/c6ra10994b
25. Lachowicz D, Kaczyńska A, Wirecka R, et al. A hybrid system for magnetic hyperthermia and drug delivery: SPION functionalized by curcumin conjugate. *Materials*. 2018;11:12. doi:10.3390/ma11122388
26. Cui Y, Yamada S. N-Cadherin Dependent Collective Cell Invasion of Prostate Cancer Cells Is Regulated by the N-Terminus of α-Catenin. *PLoS One*. 2013;8(1):e55069. doi:10.1371/journal.pone.0055069
27. Chlenski A, Nakashiro KI, Ketels KV, Korovaitseva GI, Oyasu R. Androgen receptor expression in androgen-independent prostate cancer cell lines. *Prostate*. 2001;47(1):66–75. doi:10.1002/pros.1048
28. Kulik AJ, Lekka M, Lee K, Pyka-Fościak G, Nowak W. Probing fibronectin-antibody interactions using AFM force spectroscopy and lateral force microscopy. *Beilstein J Nanotechnol*. 2015;6(1):1164–1175. doi:10.3762/bjnano.6.118
29. Singh AV, Galluzzi M, Borghi F, et al. Interaction of bacterial cells with cluster-assembled nanostructured titania surfaces: an Atomic Force Microscopy study. *J Nanosci Nanotechnol*. 2013;13(1):77–85. doi:10.1166/jnn.2013.6727
30. Singh AV, Maharjan RS, Kanase A, et al. Machine-learning-based approach to decode the influence of nanomaterial properties on their interaction with cells. *ACS Appl Mater Interfaces*. 2021;13(1):1943–1955. doi:10.1021/acsami.0c18470
31. Herman K, Lekka M, Ptak A. Unbinding kinetics of syndecans by single-molecule force spectroscopy. *J Phys Chem Lett*. 2018;9(7):1509–1515. doi:10.1021/acs.jpclett.7b03420
32. Nilsson K, Mosbach K. p-toluenesulfonyl chloride as an activating agent of agarose for the preparation of immobilized affinity ligands and proteins. *Eur J Biochem*. 1980;112(2):397–402. doi:10.1111/j.1432-1033.1980.tb07218.x